QUANTUM PHASE TRACING OF CORRELATED PHOTONS IN OPTICAL MULTIPORTS

MICHAEL RECK AND ANTON ZEILINGER
Institut für Experimentalphysik,
Universität Innsbruck, Technikerstr. 25
A–6020 Innsbruck, Austria

ABSTRACT

Multiport-beamsplitters permit experiments with photons in higher-dimensional Hilbert spaces. The classification and description of these experiments, which typically use beamsplitters, mirrors, and phase shifters, is achieved by methods borrowed from graph theory. An algorithmic approach to the calculation of the unitary matrix for an arbitrary arrangement of these components is introduced. As an example, the two-photon correlations in a generalized Franson type experiment using three-way beamsplitters are calculated.

1 Introduction

A multiport-beamsplitter can be viewed as a black box transforming n input states into n output states (see Figure 1). Thus multiports operate on photons in a higher-dimensional Hilbert space. Inside the black box we find the basic building components of a multiport experiment: beamsplitters, mirrors, and phase shifters. It seems convenient to find an abstract description of the workings of the black box as function of the parameters that can be set (internal phase shifts). A lossless experimental setup will be described by a unitary matrix.

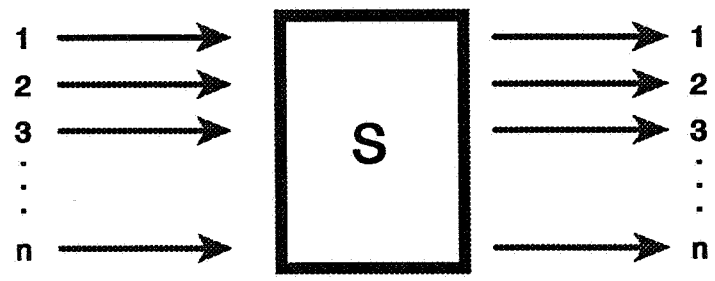

Figure 1: Any experiment with beamsplitters, mirrors, and phase shifters can be viewed as a black box. It will be described by a unitary matrix transforming n input states into n output states.

Paper presented at the Adriatico Conference on "Quantum Interferometry", Trieste, March 1993. Proceedings in Press, F. DeMartini, A. Zeilinger (Eds.), World Scientific, Singapore 1993.

2 Formal Description of Multiport Experiments

Graph theory offers a convenient way of describing the basic topological setup of an experiment. A graph consists of vertices connected by edges. In the drawing of a graph a vertex is usually represented by a point and the (directed) edges by arrows connecting the points.[1] This drawing is an abstract description of an experiment with photons (see Figure 2):

1. The experimental setup begins after the photon sources and ends before the detectors.
2. Each optical component is represented by a vertex of a directed graph.
3. All possible paths through the experimental setup to the detector are described by the graph's edges. The graph may contain loops or multiple edges. (A loop is an edge connecting a point with itself.)
4. The degree of a vertex (optical component) is the number of edges incident. Thus the degree of a mirror or phase shifter is two (one input port and one output port), the degree of a beamsplitter is four (two input ports and two output ports).
5. The properties of all optical components having only one input and one output port (mirrors, phase shifters, etc.) are taken into the graphs edges.
6. The basic building block is the *beamsplitter*. The properties of the beamsplitters (complex reflectivity and transmittivity) are attached to the vertices of the graph.
7. Each beamsplitter must have four ports, therefore all "dangling" edges (i.e. external input and output ports of the system) can be left away in the drawing. Thus the number edges incident on each beamsplitter represented by a dot in the graph must be thought supplemented by edges not connected to other beamsplitters, making a total of four ports (see Figure 2).

Once the graph of an experiment is drawn it is easy to formalize its description. The experimental setup can be described by a matrix S transforming the probability amplitudes at the n input ports into the amplitude at the n output ports. The matrix is unitary if the setup is lossless.

3 Quantum Phase Tracing

The calculation of the unitary transform matrix is accomplished by "quantum phase tracing". All possible paths from the sources to the detectors are traced through the graph. The phases along the edges are summed up and the resulting probability amplitudes of indistinguishable alternative paths inside the experiment are added up.[2]

The detection probability at a given output is proportional to the absolute square of the probability amplitude.

The graph is the fingerprint of the experimental setup. Isomorphic graphs belong to equivalent experimental setups. Graph theory provides a list of all possible graphs with a given number of edges and vertices. Thus we can list all non-equivalent experimental setups with a given number of beamsplitters (see Figure 2).

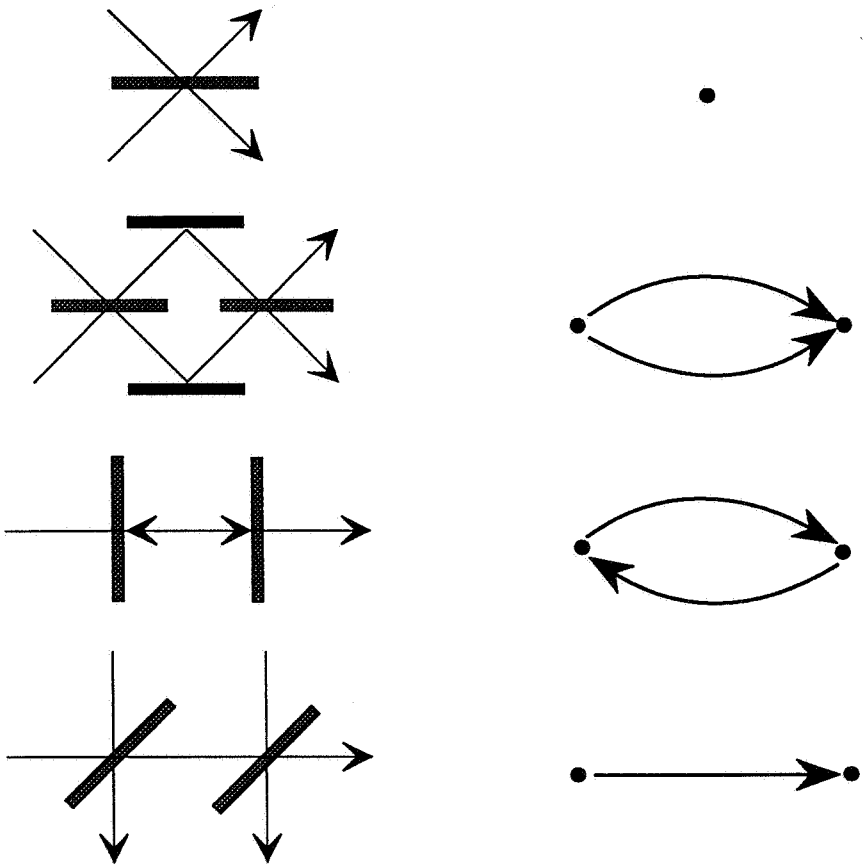

Figure 2: All possible setups with one and two beamsplitters and their corresponding graphs: a single beamsplitter, a Mach-Zehnder interferometer, a Fabry-Pérot interferometer, and a three-way beamsplitter. Each dot in the graph represents a beamsplitter and must be thought supplemented by "dangling" edges (i.e. the external input and output ports) to give a total of two input and two output ports at each beamsplitter.

Quantum phase tracing in the frequency domain assumes all phase shifts are frequency dependent. This gives the system matrix of the experimental setup as a function of the vertices (beamsplitters) and the edges (phase shifts). The frequency-dependent system matrix is then integrated over the input wave packet profile giving the time-dependent output amplitudes.[3,5]

Scattering matrix methods can be used to calculate the system's unitary matrix.[6]

4 Calculating the System Matrix

The system matrix relates the output probability amplitudes with the input:

$$\vec{a}_{\text{out}} = S\vec{a}_{\text{in}}. \tag{1}$$

The system matrix describes the external outputs connected to the detectors as a function of the external inputs which are connected to the sources. It contains two contributions. One describes the scattering at the beamsplitters; the other the propagation between connected beamsplitters. Each beamsplitter may have internal and external ports. The internal ports are those which are connected to another beamsplitter in the system. The number of external ports is equal to the dimension of the system's unitary matrix.

The scattering matrix describing the vertices of the graphs (beamsplitters) can be build from block matrices describing the transfer from internal and external inputs of the beamsplitters to their internal and external outputs:[6]

$$\begin{pmatrix} \vec{a}_{\text{out}}(ext) \\ \vec{a}_{\text{out}}(int) \end{pmatrix} = \begin{bmatrix} S_{ee} & S_{ei} \\ S_{ie} & S_{ii} \end{bmatrix} \begin{pmatrix} \vec{a}_{\text{in}}(ext) \\ \vec{a}_{\text{in}}(int) \end{pmatrix} \tag{2}$$

The submatrix S_{ei}, for example, describes the scattering from the internal inputs of the beamsplitters to the external outputs. The connection matrix Γ describes the propagation between beamsplitters, that is the edges of the graph (with phase shifts):

$$\vec{a}_{\text{out}}(int) = \Gamma\, \vec{a}_{\text{in}}(int). \tag{3}$$

Solving equations (2) and (3) for the external ports gives an expression for the system matrix:

$$\vec{a}_{\text{out}} = \left[S_{ee} + S_{ei}\left(\Gamma - S_{ii}\right)^{-1} S_{ie}\right] \vec{a}_{\text{in}} \tag{4}$$

5 Example: Three-Way Beamsplitter

The experimental setup for a three-way beamsplitter and the corresponding graph are shown in Figure 3.

Each vertex in the graph (simple beamsplitter X with reflectivity r_X and transmittivity t_X) is described by a 2×2 matrix[4,5]:

$$\begin{pmatrix} x_3 \\ x_4 \end{pmatrix} = \begin{bmatrix} t_X & ir_X \\ ir_X & t_X \end{bmatrix} \begin{pmatrix} x_1 \\ x_2 \end{pmatrix} \tag{5}$$

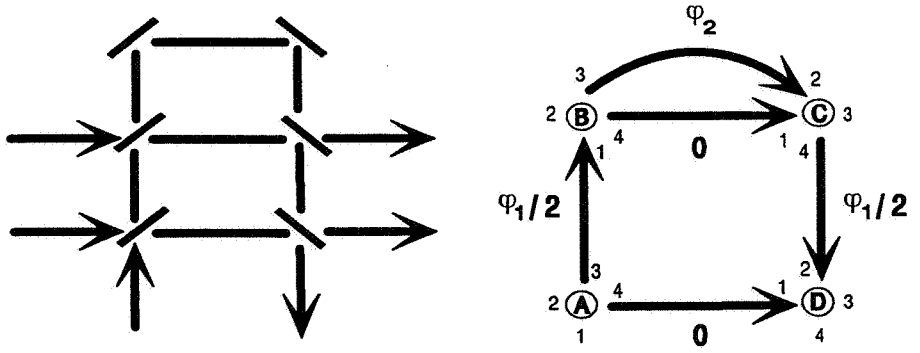

Figure 3: Experimental setup and graph for a three-way beamsplitter. External input ports: A_1, A_2, B_2; Internal input ports: B_1, C_1, C_2, D_1, D_2; External output ports: C_3, D_3, D_4; Internal output ports: A_3, A_4, B_3, B_4, C_4.

The inputs of each beamsplitter are numbered 1 and 2; the outputs are numbered 3 and 4. The scattering matrix for the three-way beamsplitter is given by

$$\left(\begin{array}{c} C_3 \\ D_3 \\ D_4 \\ \hline A_3 \\ A_4 \\ B_3 \\ B_4 \\ C_4 \end{array}\right) = \left[\begin{array}{ccc|ccccc} 0 & 0 & 0 & 0 & t_C & ir_C & 0 & 0 \\ 0 & 0 & 0 & 0 & 0 & 0 & t_D & ir_D \\ 0 & 0 & 0 & 0 & 0 & 0 & ir_D & t_D \\ \hline t_A & ir_A & 0 & 0 & 0 & 0 & 0 & 0 \\ ir_A & t_A & 0 & 0 & 0 & 0 & 0 & 0 \\ 0 & 0 & ir_B & t_B & 0 & 0 & 0 & 0 \\ 0 & 0 & t_B & ir_B & 0 & 0 & 0 & 0 \\ 0 & 0 & 0 & 0 & ir_C & t_C & 0 & 0 \end{array}\right] \left(\begin{array}{c} A_1 \\ A_2 \\ B_2 \\ \hline B_1 \\ C_1 \\ C_2 \\ D_1 \\ D_2 \end{array}\right) \tag{6}$$

The connection matrix for the three-way beamsplitter is

$$\left(\begin{array}{c} A_3 \\ A_4 \\ B_3 \\ B_4 \\ C_4 \end{array}\right) = \left[\begin{array}{ccccc} e^{-i\varphi_1/2} & 0 & 0 & 0 & 0 \\ 0 & 0 & 0 & 1 & 0 \\ 0 & 0 & e^{-i(\varphi_2+\pi)} & 0 & 0 \\ 0 & 1 & 0 & 0 & 0 \\ 0 & 0 & 0 & 0 & e^{-i\varphi_1/2} \end{array}\right] \left(\begin{array}{c} B_1 \\ C_1 \\ C_2 \\ D_1 \\ D_2 \end{array}\right) \tag{7}$$

A common phase in the connection matrix has been set to zero.

For B and C as 50% beamsplitters, A and D as 66.67% beamsplitters, the multiport has the following system matrix S relating input states with output states:

$$\left[\begin{array}{ccc} i\frac{e^{i\varphi_1/2}(1-e^{i\varphi_2})}{2\sqrt{3}} & \frac{e^{i\varphi_1/2}(e^{i\varphi_2}-1)}{\sqrt{6}} & \frac{1+e^{i\varphi_2}}{2} \\ i\frac{2-e^{i\varphi_1}-e^{i(\varphi_1+\varphi_2)}}{3\sqrt{2}} & \frac{1+e^{i\varphi_1}+e^{i(\varphi_1+\varphi_2)}}{3} & \frac{e^{i\varphi_1/2}(e^{i\varphi_2}-1)}{\sqrt{6}} \\ -\frac{4+e^{i\varphi_1}+e^{i(\varphi_1+\varphi_2)}}{6} & i\frac{2-e^{i\varphi_1}-e^{i(\varphi_1+\varphi_2)}}{3\sqrt{2}} & i\frac{e^{i\varphi_1/2}(1-e^{i\varphi_2})}{2\sqrt{3}} \end{array}\right] \tag{8}$$

6 One Photon Description

The photon at input port l of the multiport is described by wave-packet creation operator $\hat{a}_l^\dagger(\omega)$ which creates a photon with a frequency distribution $\epsilon_l(\omega)$:[3,5]

$$\hat{A}_l^\dagger(\alpha) := \int_0^\infty \epsilon_l(\omega)\hat{a}_l^\dagger(\omega)d\omega \tag{9}$$

$$\alpha_l(t) = \frac{1}{\sqrt{2\pi}}\int_0^\infty \epsilon_l(\omega)e^{-i\omega t}d\omega \tag{10}$$

The function $\alpha_l(t)$ gives the probability amplitude for photon detection with a detector placed at input port l before the system.

A coherent superposition of photon states at the input ports l results in a probability amplitude after the system given by

$$\alpha_m(t) = \frac{1}{\sqrt{2\pi}}\sum_l \int_0^\infty S_{ml}(\omega)\,\epsilon_l(\omega)e^{-i\omega t}d\omega$$

with S_{ml} the matrix element relating a specific input port l with a specific output port m.

7 Two-Photon Description

Now we consider the case of two photons propagating through two systems (e.g. see Figure 4). The two photon wave-packet creation operator is:[3]

$$\hat{K}^\dagger(\zeta) := \int_0^\infty\int_0^\infty \zeta(\omega_1,\omega_2)\,\hat{a}_1^\dagger(\omega_1)\hat{a}_2^\dagger(\omega_2)d\omega_1\,d\omega_2 \tag{11}$$

with a normalized joint wave-packet profile.

$$\int_0^\infty\int_0^\infty |\zeta(\omega_1,\omega_2)|^2 d\omega_1 d\omega_2 = 1 \tag{12}$$

If the two photons are directed into separate multiports the coincidence probability during the time T (coincidence window) is the integral over the second order correlation function $G^{(2)}_{1'2'}(t_1,t_2)$ describing the correlation at detectors $1'$ and $2'$ placed after the multiports.

$$P_{1'2'}(T) = \eta^2 \int_{-T/2}^{T/2}\int_{-T/2}^{T/2} G^{(2)}_{1'2'}(t_1,t_2)\,dt_1\,dt_2 \tag{13}$$

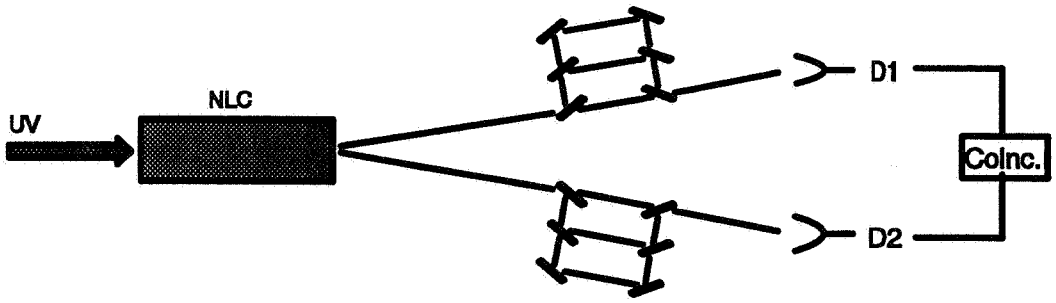

Figure 4: Two photons from a parametric downconversion source are directed into separate multiports and detected in coincidence.

The photodetectors at the output ports have an efficiency η. The second order correlation function is given by:

$$G^{(2)}_{1'2'}(t_1,t_2) = \left| \int_0^\infty \int_0^\infty S_{1'1}(\omega_1) S_{2'2}(\omega_2) \zeta(\omega_1,\omega_2)\, e^{-i(\omega_1 t_1 + \omega_2 t_2)} d\omega_1\, d\omega_2 \right|^2 \qquad (14)$$

with $S_{1'1}(\omega_1)$ and $S_{2'2}(\omega_2)$ the matrix elements relating the respective input and output ports.

8 Two-Photon Coincidence Experiment with Two Three-Way Beamsplitters

We consider two three-way beamsplitters as described above. Signal and idler photons from a parametric downconversion source are fed into input ports A_2 and A_2'. This experiment is a generalized form of that suggested by Franson.[7] In the present case three possible paths can be brought to interference. For simplicity we consider the degenerate case $\omega_s = \omega_i = \omega_p/2$ and two identical three-way beamsplitters (see Figure 4). The parameters that can be varied are the phase shifts φ_1 and φ_2. The UV pump wave is considered ideally monochromatic.[8] We assume the filters have equal bandwidth σ and centers $\omega_0 = \omega_p/2$ before the detectors.

1. If $\varphi_1 \ll \sigma T \ll \omega_0 T$ and $\varphi_2 \ll \sigma T \ll \omega_0 T$, that is the path differences are much less than the filter bandwidths and much less than the detector response times T, the probability for coincidence counts is

$$P_{12}^{\Psi} = \frac{1}{81}\left[3 + 2\cos(\varphi_1) + 2\cos(\varphi_2) + 2\cos(\varphi_1+\varphi_2)\right]^2 \qquad (15)$$

The coincidence probability is the square of the single-photon detection probability and we see single-photon interference fringes with visibility 1.

This is a consequence of the fact that for small enough path differences in the interferometers the time of detection of one photon does not provide information about the path taken by either photon.

2. If $\sigma T \ll \omega_0 T \ll \varphi_1$ and $\sigma T \ll \omega_0 T \ll \varphi_2$, that is the path differences are much greater than the filter bandwidths and much greater than the detector response times T, the probability for coincidence counts then is

$$P_{12}^{\Psi} = \frac{1}{81}\left[3 + 2\cos(2\varphi_1) + 2\cos(2\varphi_2) + 2\cos(2\varphi_1 + 2\varphi_2)\right] \qquad (16)$$

   We observe two-photon interference fringes with visibility 1.

In the second case the coincidence window is so narrow that the second photon's arrival time can be used to determine the path take by the first photon in the other interferometer. Thus there can be no single-photon interference. Detection in coincidence, on the other hand, destroys the two-photon path information, that is the three possible combinations long-long, medium-medium, and short-short are indistinguishable and can interfere. This is a direct result of the entanglement of the two-photon wavefunction.

References

1. F. Harary, Graph Theory, (Addison-Wesley, Reading, Massachusetts, 1969).
2. R. P. Feynman, R. B. Leighton, and M. Sands, *The Feynman Lectures on Physics*, vol. III, (Addison-Wesley, Reading, Massachusetts, 1964).
3. R. A. Campos, B. E. A. Saleh, and M. C. Teich, Phys. Rev. A **42**, 4127 (1990).
4. A. Zeilinger, Am. J. Phys. **89**, 882–883 (1981)
5. H. Fearn and R. Loudon, J. Opt. Soc. Am. B **6**, 917 (1989).
6. J. A. Dobrowolski, *Introduction to Computer Methods for Microwave Circuit Analysis and Design*, (Artech House, Boston, 1991).
7. J. D. Franson, Phys. Rev. Lett. **62**, 2205 (1989).
8. M. Horne, A. Shimony, and A. Zeilinger, "Down-conversion photon pairs: a new chapter in the history of quantum mechanical entanglement," in *Quantum Coherence*, edited by J. S. Anandan, pp. 356–372, (World Scientific, Singapore, 1990).

Acknowledgements

This work was supported by the Fond zur Förderung der Wissenschaftlichen Forschung, Austria, *Schwerpunkt Quantenoptik* project number S6502 and by the U.S. NSF grant PHY 92-13964.